of pattern formation by swimming microorganisms. J. Protozool. **22:** 296–306.

MACNAB, R. M. 1987. Motility and chemotaxis, p. 732–759. *In* F. C. Neidhardt [ed.], *Escherichia coli* and *Salmonella typhimurium*: Cellular and molecular biology 1. Am. Soc. Microbiol.

MARGALEF, R., M. ESTRADA, AND D. BLASCO. 1979. Functional morphology of organisms involved in red tides, as adapted to decaying turbulence, p. 89–94. *In* Toxic dinoflagellate blooms. Proc. 2nd Int. Conf. Elsevier-North Holland.

MARSHALL, H. G. 1984. Phytoplankton distribution along the eastern coast of the USA. Part 5. Seasonal density and cell volume patterns for the northeastern continental shelf. J. Plankton Res. **6:** 169–193.

MITCHELL, J. G. 1988. Microplankton live in a structured environment. Ph.D. thesis, State Univ. New York, Stony Brook. 233 p.

———, A. OKUBO, AND J. A. FUHRMAN. 1985. Microzones surrounding phytoplankton form the basis for a stratified marine microbial ecosystem. Nature **316:** 58–59.

OKUBO, A. 1971. Horizontal and vertical mixing in the sea, p. 89–168. *In* D. W. Hood [ed.], Impingement of man on the oceans. Wiley-Interscience.

PEDLEY, T. J., N. A. HILL, AND J. O. KESSLER. 1988. The growth of bioconvection patterns in a uniform suspension of gyrotactic micro-organisms. J. Fluid Mech. **195:** 223–237.

RICHARDSON, L. L., C. AGUILAR, AND K. H. NEALSON. 1988. Mn oxidation in pH and O_2 microenvironments produced by phytoplankton. Limnol. Oceanogr. **33:** 352–363.

ROBERTS, A. M. 1981. Hydrodynamics of protozoan swimming, p. 5–65. *In* M. Levandowsky and S. H. Hutner [eds.], Biochemistry and physiology of protozoa. V. 4, 2nd ed. Academic.

SIGGIA, E. D. 1981. Numerical study of small-scale intermittency in three-dimensional turbulence. J. Fluid Mech. **107:** 375–406.

TENNEKES, H., AND J. L. LUMLEY. 1972. A first course in turbulence. MIT.

Submitted: 21 June 1988
Accepted: 14 June 1989
Revised: 1 November 1989

Limnol. Oceanogr., 35(1), 1990, 130–136

Fractal geometry of marine snow and other biological aggregates

Abstract—Fractal dimensions of aggregates can potentially be used to classify aggregate morphology as well as to identify coagulation mechanisms. Microbial aggregates of *Zoogloea ramigera* have a cluster fractal dimension of 1.8±0.3 (±SD), suggesting that these aggregates are formed through cluster-cluster coagulation. An analysis of size-porosity correlations for two types of marine snow aggregates yielded fractal dimensions of 1.39±0.06 and 1.52±0.19, which were lower than values describing inorganic colloidal aggregation.

Large, amorphous aggregates, known as marine snow, compose the largest component of mass sedimenting through the water column (Fowler and Knauer 1986). These aggregates consist of diatoms, bacteria, fecal pellets, cast houses of appendicularians, and nearly all other microscopic organic and inorganic matter present in the ocean. The manner in which these larger aggregates are formed is not well understood. The growth of microaggregates (<0.5 mm) and marine snow-sized aggregates (>0.5 mm) can result from Brownian motion, eddy diffusion, shear coagulation, and differential sedimentation, as well as through growth of organisms within the aggregate microhabitat. McCave (1984) has calculated that shear rates in the ocean are too low to account for observed, steady state particle size distributions. Although this conclusion implies that physical mechanisms of aggregate formation are less important than biological mechanisms in marine systems, marine snow aggregates have macroscopic morphologies that are characteristic of inorganic aggregates formed through physical coagulation mechanisms. This similarity, which

Acknowledgments

This work was supported by the Donors of The Petroleum Research Fund (administered by the American Chemical Society) and ONR contract N00014-88-K0387.

can be established with fractal geometry (Mandelbrot 1977; Feder 1988), provides evidence that aggregates can form in the ocean through physical coagulation.

The structures of inorganic aggregates, such as gold particle clusters formed irreversibly in suspension, are scale invariant or fractal (Witten and Cates 1986). The number of particles, N, in a fractal aggregate is

$$N \sim l^{D_n} \quad (1)$$

where D_n is the cluster fractal dimension determined for the object in n dimensions, and l is the characteristic length scale of the aggregate. For a Euclidean object such as a sphere, $D_3 = 3$. Aggregates formed by random processes have fractal dimensions significantly less than the Euclidean 3. Computer simulation of aggregate growth by random processes indicates that the magnitude of the fractal dimension is determined by the mechanism of aggregate growth. Aggregates formed through the addition of particles into the cluster one at a time (particle-cluster) have three-dimensional fractal dimensions in the range of 2.5–3.0 (Schaefer 1989). Aggregates formed through collision of clusters (cluster-cluster) have lower fractal dimensions, typically with $1.6 \leq D_3 \leq 2.2$ (Witten and Cates 1986).

Recent research on inorganic colloidal aggregation has demonstrated a relationship between aggregate structure and cluster-cluster aggregation kinetics (Lin et al. 1989). Computer simulations and experiments with several types of colloids indicate that two different types of aggregates form as a function of different particle stickiness or different collision efficiencies (Table 1). As the probability of attachment on collision approaches unity, particles stick upon contact, forming highly tenuous structures. This pattern results in very rapid coagulation, referred to as diffusion-limited colloidal aggregation (DLCA) because the rate of aggregate growth is limited by particle transport. The highly tenuous structure is a result of very sticky particles moving in a random walk; particles cannot penetrate the aggregate since they attach to particles with which they collide on the aggregate exterior. Aggregates formed through DLCA are characterized by fractal dimensions around 1.8. As the attachment probability approaches zero, particles may collide many times before sticking, allowing them to penetrate the aggregate and increasing the aggregate density. This aggregation is classified as reaction-limited colloidal aggregation (RLCA) and results in aggregates with D_3 values around 2.1.

Table 1. Fractal dimensions of inorganic colloids formed through either DLCA or RLCA (data from Lin et al. 1989).

Colloid	DLCA	RLCA
Gold	1.86	2.14
Silica	1.85	2.07
Polystyrene	1.82	2.09

The occurrence of two distinct regimes of colloidal aggregation suggests that fractal scaling relationships can potentially identify the aggregate formation mechanism as well as the attachment efficiency of particles composing the aggregate. Lin et al. (1989) demonstrated universality of fractal classification for inorganic systems with colloidal gold, silica, and polystyrene. It has not been established, however, that biological aggregates can be similarly classified. Most microorganisms grown in batch culture aggregate during late log growth (Calleja 1984). This aggregation creates a more complex system than previously examined for inorganic coagulation because particles (daughter cells) can be produced during coagulation. Microbial growth occurs during aggregation, so we would expect biological aggregates to have D_3 values that are between values reported for particle-cluster and cluster-cluster models. The size of the microbial aggregates and the range of coagulation mechanisms (e.g. shear, differential sedimentation), however, create conditions far different from systems previously characterized by fractal analysis.

In order to establish that biological aggregates have fractal structures similar to inorganic aggregates, we developed microbial aggregates composed of homogeneously sized particles with pure cultures of microorganisms. We grew aggregates of *Zoogloea ramigera* type I-16-M (ATCC-19623), a rod-shaped, gram-negative bac-

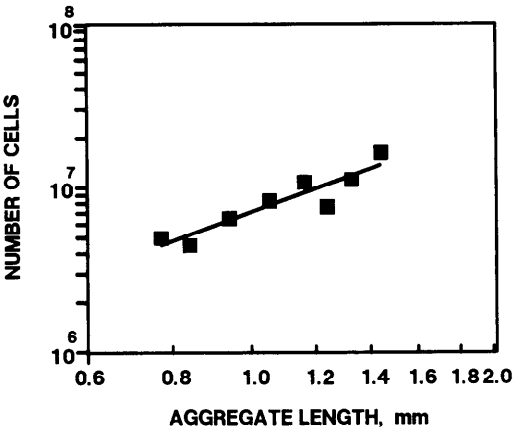

Fig. 1. Cells per floc of *Zoogloea ramigera* (■) with a regression line through the data ($r^2 = 0.87$) indicating $D_3 = 1.8 \pm 0.3$ (± 1 SD). Data points represent averages of 3–6 aggregates.

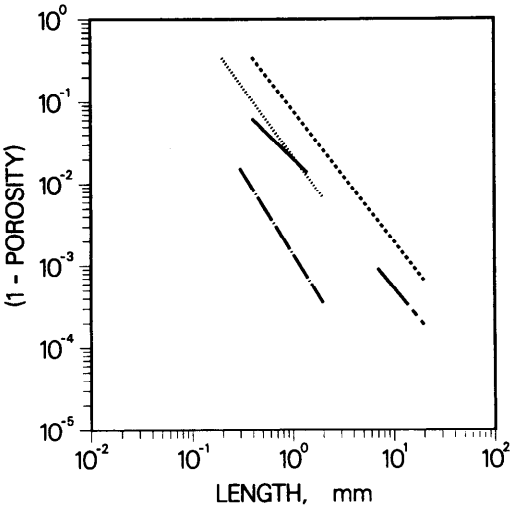

Fig. 2. Occupied volume (1 − porosity) correlations with aggregate size for several different types of biological aggregates from both natural and engineered environments: *Zoogloea ramigera* (——); marine snow (– – –); diatom flocs (– –); normal wastewater bioreactor flocs (· · · · ·); filamentous wastewater bioreactor flocs (– · – · –).

terium which attaches with cellulosic fibers that resist floc breakage during aggregate-sizing experiments. Suspended cultures (15 ml) were developed at room temperature (23°C) on nutrient broth (Difco) in 36-ml test tubes clamped to a laboratory rotator. After 24 h, cultures were poured into a sterile Petri dish and diluted with sterile water to increase floc separation. Individual aggregates of *Z. ramigera* were captured in ~20 μl of media with a 100-μl pipette with the plastic tip cut between the 25- and 50-μl markings and transferred to a 2-ml drop of solution to aid separation of flocs from free-living cells. The pipet tip was then rinsed with sterile water and the aggregate transferred to a well slide. Flocs were viewed with direct light microscopy (10× power, Olympus model BH-2) to determine the largest aggregate length and to sketch the aggregate.

The number of cells composing each microscopically sized aggregate was determined by rinsing the slide contents into a sterile, acid-washed vial and adding sterile water for a final volume of 1 ml. The floc was dispersed enzymatically with 10 mg ml^{-1} of cellulase (Sigma Chemical No. C-7377), vortexing the solution for 1 min, and placing the vials in a rotator. Samples were preserved with 2% formaldehyde and counted with acridine orange epifluorescence (Hobbie et al. 1977). Samples containing incompletely dispersed flocs were discarded. Transfer of culture material without flocs through the above sequence of steps was used to verify that free-living cells included with the floc transfer were a negligible portion of the total counts.

Fractal aggregates are characterized by large spatial and sample-to-sample fluctuations in properties (Meakin 1988). Therefore, we sized 47 aggregates by longest length and averaged all aggregates within 0.1-mm size classes spanning 0.7–1.5 mm long. From a log-log regression with Eq. 1 and data shown in Fig. 1, we determined a fractal dimension for *Z. ramigera* flocs of 1.8 with a standard error of 0.3 ($r^2 = 0.87$, $n = 8$) based on the longest aggregate length. This value is much smaller than the Euclidean value of $D_3 = 3$ expected for spherical aggregates and is experimental evidence of the three-dimensional fractal structure of these aggregates. The magnitude of this fractal dimension is within the range indicated for aggregates formed through cluster-cluster coagulation, but is not sufficiently precise to identify whether cluster formation is within the range expected for diffusion- or reaction-limited aggregation.

Several investigators have related the po-

Table 2. Fractal dimensions of biological aggregates determined from empirical size-porosity equations.

Biol. aggregate type	Size range (mm)	Fractal dimension	References
Marine snow			
General	0.4–20	1.39±0.15*	Alldredge and Gotschalk 1988
Diatom	7–20	1.52±0.19*	Logan and Alldredge 1989
Bioreactor			
Normal	0.2–2	1.3	Tambo and Watanabe 1979
Filamentous	0.3–2	1.0	Tambo and Watanabe 1979
Zoogloea ramigera	0.4–1.4	1.8±0.3*	This study

*±1SD.

rosity, p, of biological aggregates to aggregate size (Tambo and Watanabe 1979; Alldredge and Gotschalk 1988; Logan and Alldredge 1989) with

$$1 - p = al^b \tag{2}$$

where a and b are empirical constants, and b is negative. Porosity has been determined either directly from gravimetry, assuming an average particle density (Alldredge and Gotschalk 1988; Logan and Alldredge 1989) or indirectly from settling experiments (Tambo and Watanabe 1979). If the number of particles or cells comprising the aggregate is known, the porosity can be directly calculated from

$$1 - p = \frac{NV_c}{V} \tag{3}$$

where V_c is the average volume of cells composing the aggregate and V the volume occupied by an aggregate. Following convention (Witten and Cates 1986; Li and Ganczarczyk 1987; Logan and Alldredge 1989), we defined the volume of *Z. ramigera* aggregates as the volume of a sphere just capable of enclosing the aggregate. Combining Eq. 1 and 3, we obtained the fractal relationship

$$(1 - p) \sim l^{D_3 - 3}. \tag{4}$$

A comparison of Eq. 2 and 4 shows that $D_3 = 3 + b$. Therefore, the fractal dimension of marine snow, as well as other types of biological aggregates, can be estimated with published size-porosity relationships.

Although marine snow aggregates can be much larger than other types of biological aggregates, they are denser than aggregates of similar size (Fig. 2). The porosities determined for *Z. ramigera* aggregates by our microscopic methods are similar to porosities determined for aggregates normally found in wastewater treatment bioreactors. On occasion, filamentous cells become numerically abundant in these bioreactors. This produces highly filamentous flocs that are morphologically different from normal bioreactor flocs that consist primarily of clumps of spherical or rod-shaped cells. These filamentous flocs are much more porous than normal bioreactor flocs.

The fractal dimensions for both naturally occurring and engineered reactor aggregates are in the range of 1.0–1.5 (Table 2). *Zoogloea ramigera* aggregates grown in the laboratory had the largest fractal dimension of all aggregates examined. This result indicates that aggregates grown in the laboratory are more compact, having higher fractal dimensions than aggregates formed in the ocean.

Fractal dimensions have been calculated with settling data (Li and Ganczarczyk 1989). These fractal dimensions, however, contain a mixture of scaling properties. From a force balance on a settling particle, we have (Bird et al. 1960)

$$V(\rho - \rho_f)g = 0.5A\rho_f C_D U^2 \tag{5}$$

where ρ is the floc density, ρ_f the fluid density, g the gravitational constant, A the projected surface area of the floc perpendicular to direction of settling, C_D a drag coefficient, and U the aggregate settling velocity. For small aggregates, the drag coefficient is proportional to aggregate settling velocity and inversely proportional to aggregate length. For a solid object, such as a sphere with diameter d, $C_D = 24/\mathrm{Re}$ for $\mathrm{Re} = Ud/\nu \ll$

Table 3. Fractal dimensions of biological aggregates determined from settling velocity data.

Biol. aggregate type	Size range (mm)	Fractal dimension	References
Marine snow (in situ)	7–20	1.26±0.06*	Alldredge and Gotschalk 1988
Estuarine	0.02–2	1.78	Gibbs 1985
Lacustrine	0.012–0.04	1.39–1.69	Hawley 1982
Oceanic	~0.1	2.14	
Oceanic	~0.4	1.94	
Recoagulated oceanic sediments	0.1–1	1.57	Kajihara 1971

*±SD.

1 where ν is the fluid kinematic viscosity. Using this drag coefficient in Eq. 5, we obtain

$$U = \frac{V(\rho - \rho_f)d}{12A\rho_f\nu}. \quad (6)$$

$$(\rho - \rho_f) = (1 - p)(\rho_c - \rho_f)$$

where ρ_c is the density of the particles comprising the aggregate, so we can define a proportionality between settling velocity and aggregate geometry as

$$U \sim \frac{V(1 - p)d}{A}. \quad (7)$$

For a spherical, solid object with Re $\ll$ 1, $U \sim d^2$, in agreement with Stokes' law (Bird et al. 1960).

We can define a proportionality for a fractal object by combining Eq. 1, 3, and 7, to obtain

$$U \sim l^{D_3+1-D_2} \quad (8)$$

where we have assumed that $A \sim l^{D_2}$, with D_2 the two-dimensional fractal dimension that relates the projected surface area to the largest aggregate length. Li and Ganczarczyk (1989) have defined the scaling power in Eq. 8 as a single fractal dimension. This scaling power is a function of aggregate geometry in both two and thee dimensions and is defined here as a fractal dimension, $D(2)$, without a subscript. The number in parentheses indicates the value of this fractal dimension for a solid object. The fractal dimension D_3 can be estimated with settling velocity data from $D_3 = D(2) - 1 + D_2$, and by assuming that $D_2 \simeq 2$.

Values of D_3 obtained from Eq. 8 and settling data span a wide range of 1.26–2.14 (Table 3). Many of these values are below those expected for cluster-cluster coagulation. Our estimate of D_3 is exact for any self-similar object (Euclidean or fractal) if a geometric length scale is used to define the aggregate area. If longest length is used, then $D_2 \leq 2$, and the calculated value of D_3 is an upper estimate of the true value. Other factors may influence the relationship between D_3 and $D(2)$. For example, the marine snow aggregates examined by Alldredge and Gotschalk (1988) extend beyond the creeping flow range and have Reynold's numbers greater than unity. The low value of D_3 = 1.26 may result from exceeding the length scales applicable to smaller aggregates. This lower value also may be related to the fact that aggregates examined by Alldredge and Gotschalk were examined in situ and therefore were not disrupted by handling. The value of $D_3 = 1.26 \pm 0.06$ (±SD) obtained from the settling velocity data of Alldredge and Gotschalk is slightly lower than the value of $D_3 = 1.39 \pm 0.15$ (±SD) calculated from their gravimetric analysis. This finding suggests that settling velocity correlations may underestimate D_3 values.

Most of the D_3 values calculated for marine snow are smaller than the range of values observed for inorganic aggregates formed through diffusion-limited cluster-cluster coagulation (DLCA). There have been previous reports that biological molecules exhibit different coagulation behavior than inorganic colloids (Feder et al. 1984). At the present time, we have no specific explanation for these results. It is generally accepted that aggregate characteristics are altered by fluid mixing intensity, aggregate age, and other factors not considered in our analysis (Hunt 1986). Computer simulation by Meakin (1988) demonstrated that aggregate

restructuring increases the fractal dimension. In Meakin's study, D_3 increased from 1.89 to 2.13 when long chains of an aggregate contacted and attached to other tenuous structures within the aggregate. Therefore, fluid mixing and turbulence should increase the fractal dimension. Based on our current understanding of the effect of fluid environment and coagulation kinetics, and Meakin's (1988) results, we would expect aggregates in the ocean to have higher fractal dimensions than those measured for cluster-cluster, diffusion-limited coagulation and not the lower values calculated in this study.

We have conducted some preliminary experiments on the effect of fluid environment on the fractal dimension of microbial aggregates. When we cultured *Z. ramigera* in a laboratory reactor (Omni-culture reactor, Virtis Co.) aerated at 1 liter of air min^{-1} and mixed at 160 rpm, the fractal dimension of these aggregates was 3.0 ± 0.4 ($\pm$SD) (Wilkinson 1989). This fractal dimension is essentially equal to the Euclidean three-dimensional value for a spherical object. This higher fractal dimension may be a result of more aggregate restructuring in a highly mixed vessel than occurs in less turbulent environments, such as the ocean. To date, our experiments have not had well-defined hydrodynamic environments primarily because the environments we are modeling (bioreactors and oceans) are poorly characterized with respect to fluid mixing and turbulence. Our preliminary findings, however, suggest that the fractal dimension of aggregates depends on the fluid mechanical environment.

We conclude that pure and mixed cultures of microorganisms have three-dimensional scaling properties typical of fractal structures. The magnitude of fractal dimensions of marine snow aggregates is lower than the range expected for aggregates formed by Brownian motion of colloidal aggregates and may be related to aggregate restructuring or aggregate formation through other processes, including shear coagulation and differential sedimentation. Although understanding of precisely how these factors influence aggregate characteristics is incomplete, it is hoped that fractal geometry will provide a basis for studying factors that affect the structure of biological aggregates and aggregation kinetics in natural systems.

Bruce E. Logan
Daniel B. Wilkinson

Environmental Engineering Program
Department of Civil Engineering
University of Arizona
Tucson 85721

References

ALLDREDGE, A. L., AND C. GOTSCHALK. 1988. In situ settling behavior of marine snow. Limnol. Oceanogr. **33:** 339–351.

BIRD, R. B., W. E. STEWART, AND E. N. LIGHTFOOT. 1960. Transport phenomena. Wiley.

CALLEJA, G. G. 1984. Microbial aggregation. CRC.

FEDER, J. 1988. Fractals. Plenum.

———, T. JOSSANG, AND E. ROSENQVIST. 1984. Scaling behavior and cluster fractal dimension determined by light scattering from aggregating proteins. Phys. Rev. Lett. **53:** 1403–1406.

FOWLER, S. W., AND G. A. KNAUER. 1986. Role of large particles in the transport of elements and organic compounds through the oceanic water column. Prog. Oceanogr. **16:** 147–194.

GIBBS, R. J. 1985. Estuarine flocs: Their size, settling velocity, and density. J. Geophys. Res. **90:** 3249–3251.

HAWLEY, N. 1982. Settling velocity distribution of natural aggregates. J. Geophys. Res. **87:** 9489–9498.

HOBBIE, J. E., R. J. DALEY, AND S. JASPER. 1977. Use of Nuclepore filters for counting bacteria by fluorescence microscopy. Appl. Environ. Microbiol. *33:* 1225–1228.

HUNT, J. R. 1986. Particle aggregate breakup by fluid shear, p. 85–109. *In* A. J. Mehta [ed.], Estuarine cohesive sediment dynamics. V. 14. Springer.

KAJIHARA, M. 1971. Settling velocity and porosity of large suspended particles. J. Oceanogr. Soc. Jpn. **27:** 158–162.

LI, D.-H., AND J. J. GANCZARCZYK. 1987. Stroboscopic determination of settling velocity, size and porosity of activated sludge flocs. Water Res. **21:** 257–262.

———, AND ———. 1989. Fractal geometry of particle aggregates generated in water and wastewater treatment processes. Environ. Sci. Technol. **23:** 1385–1389.

LIN, M. Y., AND OTHERS. 1989. Universality in colloid aggregation. Nature **339:** 360–362.

LOGAN, B. E., AND A. L. ALLDREDGE. 1989. The increased potential for nutrient uptake by flocculating diatoms. Mar. Biol. **101:** 443–450.

MCCAVE, I. N. 1984. Size spectra and aggregation of suspended particles in the deep ocean. Deep-Sea Res. **31:** 329–352.

MANDELBROT, B. B. 1977. Fractals: Form, chance and dimension. Freeman.

MEAKIN, P. 1988. Fractal aggregates. Adv. Colloid Interface Sci. **28:** 249–331.

SCHAEFER, D. W. 1989. Polymers, fractals and ceramic materials. Science **243:** 1023–1027.
TAMBO, N., AND Y. WATANABE. 1979. Physical characteristics of flocs 1: The floc density function and aluminum floc. Water Res. **13:** 409–419.
WILKINSON, D. B. 1989. The fractal nature of biological aggregates. M.S. thesis, Univ. Arizona. 105 p.
WITTEN, T. A., AND M. E. CATES. 1986. Tenuous structures from disorderly growth processes. Science **232:** 1607–1612.

Submitted: 5 July 1989
Accepted: 17 October 1989
Revised: 27 November 1989

Limnol. Oceanogr., 35(1), 1990, 136–143

Apparatus to determine the efficiency of transfer of bacteria from a bursting bubble to the jet drops

Abstract—An apparatus has been developed to determine the efficiency by which bacteria scavenged and attached to a bubble are transferred upon bubble bursting to the jet drops. Experiments were done by letting bubbles of 625-μm diameter rise about 27 cm through a suspension of *Serratia marcescens*. The transfer efficiency varied between 50 and 100% and was an inverse function of the concentration of bacteria in the water through which the bubbles rose.

The jet and film drops produced by air bubbles bursting at the surface of lakes, rivers, and the sea probably account for most of the aerosol generated from these waters. On a global scale this can be enormous. For example, both Blanchard (1985) and Erickson and Duce (1988) have estimated that about 10^{10} t of sea salt are cycled each year from the oceans through the atmosphere. These natural waters contain bacteria, so one should not be surprised to find bacteria in jet and film drops. What might be surprising, however, is that laboratory experiments have shown that the concentration of bacteria in jet drops can be hundreds of times that in the water in which the bubbles burst (Blanchard and Syzdek 1970; Bezdek and Carlucci 1972). Bacterial enrichment in film drops does not appear to be nearly as great as that in jet drops (Blanchard and Syzdek 1982).

It is important that an understanding of the mechanism of jet-drop bacterial enrichment be obtained, for it is possible that enrichment processes contribute to the outbreak of such respiratory diseases as legionellosis, commonly known as the Legionnaires' disease. This disease is usually associated with the aerosol produced by the bubbling and splashing of water in air-conditioning cooling towers (Dondero et al. 1980; Friedman et al. 1987). Parker et al. (1983) found in laboratory experiments that *Mycobacterium intracellulare* was enriched in jet drops and suggested that *M. intracellulare* infections in humans might be caused by a bacterial-enriched aerosol from natural waters.

The bacterial enrichment factor in jet drops is a function of the distance the bubble moves through the water before it bursts. Blanchard et al. (1981), working with bulk suspensions of *Serratia marcescens,* found that the top jet-drop enrichment factor rose linearly with the first few centimeters the bubble moved through the water before bursting at the surface, reaching a value of about 400 after only 3 cm of bubble travel. Such high enrichment factors require that bacteria collide with and stick to the surface of the rising bubble and that the transfer efficiency—the efficiency by which bacteria attached to the bubble are transferred to the jet drops—be reasonably high. The collection efficiency, defined as the efficiency by which the bacteria in the cylindrical volume swept out by a rising bubble are collected by the bubble, is very low, of the order of 0.1% (Blanchard and Syzdek 1974; Weber et al. 1983). Nothing has appeared in the

Acknowledgments
This work was supported by the National Science Foundation under grant ATM 85-14211.